

Spectral Characterization of Laser Induced Plasma from Titanium Dioxide

This article has been downloaded from IOPscience. Please scroll down to see the full text article.

2007 *Plasma Sci. Technol.* 9 456

(<http://iopscience.iop.org/1009-0630/9/4/16>)

View the [table of contents for this issue](#), or go to the [journal homepage](#) for more

Download details:

IP Address: 117.240.231.66

The article was downloaded on 12/07/2010 at 06:49

Please note that [terms and conditions apply](#).

Spectral Characterization of Laser Induced Plasma from Titanium Dioxide

V. J. DANN^{1,2}, M. V. MATHEW¹, V. P. N. NAMPOORI¹, C. P. G. VALLABHAN²,
V. M. NANDAKUMARAN¹, P. RADHAKRISHNAN¹

¹ International School of Photonics, Cochin University of Science and Technology,
Cochin 22, India

² Centre of Excellence in Lasers and Optoelectronic Sciences,
Cochin University of Science and Technology, Cochin 22, India

Abstract Optical emission from TiO₂ plasma, generated by a nanosecond laser is spectroscopically analysed. The main chemical species are identified and the spatio-temporal distribution of the plasma parameters such as electron temperature and density are characterized based on the study of spectral distribution of the line intensities and their broadening characteristics. The parameters of laser induced plasma vary quickly owing to its expansion at low background pressure and the possible deviations from local thermodynamic equilibrium conditions are tested to show its validity.

Keywords: laser induced plasma, titanium dioxide, optical emission spectroscopy, local thermodynamic equilibrium

PACS: 52.38.-r, 52.50.Jm, 52.25.Kn

1 Introduction

The interaction of laser beam with solid matter and the consequent plasma generation has been studied for many years. Despite the efforts to exploit the laser-matter interaction for material processing and diagnostic purposes by many workers, some of the aspects still need to be elucidated and clarified. In order to understand some of the characteristics of laser induced plasma (LIP) from solid targets, we have chosen titanium dioxide (TiO₂) as target. TiO₂ is a material which has importance both in areas of applied and basic sciences. This acts as a photosensitizer for photovoltaic cells and as an oxygen sensor. Pulsed laser deposition is successfully employed for thin film deposition of materials like TiO₂ and for elementary analysis^[1]. In these applications, it is important to understand the composition and the temporal as well as the spatial evolution of the species in the plasma. The conventional approach in the study of LIP is based on the assumption of local thermodynamic equilibrium (LTE) and the plasma as optically thin. Using these assumptions, parameters like the mass of plasma species, density, temperature and chemical composition of the plasma can be easily determined. In the LTE condition, Maxwell-Boltzmann and Saha relations are still locally valid. In LIP, where the fast dynamics play a fundamental role, the plasma parameters can change due to the supersonic expansion in a shorter period of time with respect to that necessary for the balance of elementary processes. The knowledge of deviations from LTE is important to understand the corrections and constraints of the theory

to be taken into account for practical applications^[2,3].

The most convenient technique, especially for the initial stages of LIP, is optical emission spectroscopy (OES), which is based on the intrinsic light emission of LIP and does not need any intrusive systems. The composition of the spectra studied at different distances from the target allows us to discuss some of the fundamental properties of LIP, which will help to understand the main processes that must be taken into account for the analysis of plasma^[4].

2 Experimental setup

A Nd:YAG laser (Spectra Physics, Quanta-Ray DCR-11) with an emission wavelength of 1064 nm was used as the source of monochromatic radiation for plasma formation inside an evacuated steel chamber. The chamber was pumped down to 2.5×10^{-5} mbar by both rotary and diffusion pumps. The laser was operated at a repetition rate of 10 Hz, with a pulse duration of 10 ns. A high resolution monochromator (1 m SPEX) coupled with a thermoelectrically cooled PMT(Photo Multiplier Tube) and a time resolved detector (gated integrator and boxcar averager, SR 250) interfaced with appropriate software were used to study the time evolution of plasma. The boxcar gate width and monochromator slit width were optimized to maximize the spectral line intensity while maintaining good temporal resolution. An aggregate of 10 signal accumulations was collected for averaging. An optical system consisting of two lenses of equal focal length was used

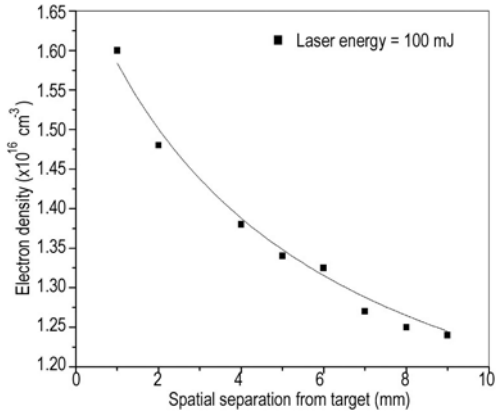


Fig.1 Spatial variation of n_e with 100 mJ of laser energy; dotted line shows the theoretical fit based on an inverse z dependence for n_e .

to produce a one-to-one image slice of the plume in a direction perpendicular to its symmetry axis. The targets were placed inside the chamber, on an axle fixed to a motorized rotating system to provide a fresh surface for ablation and an f/4.5 quartz lens was used to focus the laser beam onto the target. The detection systems were always triggered using the laser pulse. A digitizing fast oscilloscope (LeCroy 6050 A, 500 MHz) was used to calibrate and control the gate width and time delay after the laser irradiation. A CCD detector (Roper Scientific, NTE/CCD-1340/100- EM) coupled to the exit port of a spectrograph (Acton Research, SpectraPro 500i) was used to record the spectral details collected for the time integrated measurements. Studies of LIP from TiO_2 were made at various power levels of the pump laser.

3 Results and discussion

During the evolution of laser induced plasma, excitation and ionization of the evaporated material occur so that the depositing material is energetically suitable for the film formation. It is then important to determine the thermodynamic parameters of LIP such as electron number density (n_e) and electron temperature (T_e). The emission spectra of LIP have been observed at different distances from the target and different delay times (t) with respect to the laser pulse. Our interest is mainly concentrated on the initial high density plasma evolution ($t \leq 300$ ns). We have chosen spectral lines of Ti I and Ti II for plasma diagnostics. The detection of Stark broadening and displacement of spectral lines allow estimating n_e , without considering LTE. The full width at half maximum (FWHM) of a Stark broadened line (in nm), without an ionic contribution is given by the simple relation,

$$\Delta\lambda_{\frac{1}{2}} = 2w(n_e/10^{16}) \text{ nm}, \quad (1)$$

where w is the electron impact parameter^[5,6].

The line emission from Ti II (350.5 nm) is used to evaluate n_e as a function of space and time. The value

Table 1. Selected spectral lines and corresponding spectral data of upper excitation levels

Wavelength (nm)	$A(\text{s}^{-1})$	g_m	Species	$E_m(\text{eV})$
346.1	6.27×10^6	10	Ti II	3.71
348.4	9.7×10^7	8	Ti II	7.85
350.5	6.5×10^5	10	Ti II	5.42

of n_e exhibits a rapidly decreasing behaviour (from $1.6 \times 10^{16} \text{ cm}^{-3}$ at 1 mm to $1.2 \times 10^{16} \text{ cm}^{-3}$) for distances up to 9 mm from the target surface, as shown in Fig. 1. Its variation with distance perpendicular to the target (z) approximately follows an inverse dependence on z , which indicates that the initial expansion of the plume is one dimensional and is in agreement with the plume expansion model given by SINGH et al^[7]. In the present work also, the given n_e distribution fits in well with an inverse z dependence of the type $n_e = c + b/(z + a)$ with $a \approx 5$, $b \approx 4$ and $c \approx 1$. A series of emissions from Ti I are also analysed for spectral broadening due to Stark effect. Both the emissions from Ti I and Ti II show the same spatial variation. The Stark broadening parameter (w) for Ti I (586.5 nm) is not reported. From the value of n_e obtained through the studies on Ti II line, we can evaluate w in respect of the Ti I line. The parameter w thus obtained has the same order of magnitude as reported in Ref. [5].

A time integrated measurement is made to evaluate the spatial variation of electron temperature from the target. The measured distribution functions can be represented in a Boltzmann form with a good approximation. Assuming a Boltzmann distribution, the plasma temperature can be determined by Boltzmann plot technique using the measurements of spectral intensities (I_{mn}) by the following equation, representing an energy transition from an upper energy state m to a lower state n :

$$\ln\{[I_{mn}\lambda_{mn}]/[A_{mn}g_m]\} = \ln\{N/2\} - \{E_m/kT_e\}. \quad (2)$$

The parameter λ_{mn} is the transition wavelength, A_{mn} is the transition probability, E_m and g_m are the energy and statistical weight of the upper level respectively. The temperature is obtained from the slope of the plot of $\ln\{[I_{mn}\lambda_{mn}]/[A_{mn}g_m]\}$ vs E_m . We have chosen three transitions of Ti II with well separated upper energy levels in order to determine kT_e . The selected transitions along with their characteristic parameters are listed in Table 1.

The spatial variation of the electron temperature shown in Fig. 2 is typical with a rapid decay near the target and a slowly varying function of space at larger distances. The lowering of the decay rate of temperature at larger distances is mainly due to the energy gained from three body recombination that compensates for the expansive cooling^[8]. The calculations are based on the assumption that the emitting species are in collision equilibrium with the electrons and self-absorption for the spectral lines chosen are neglected.

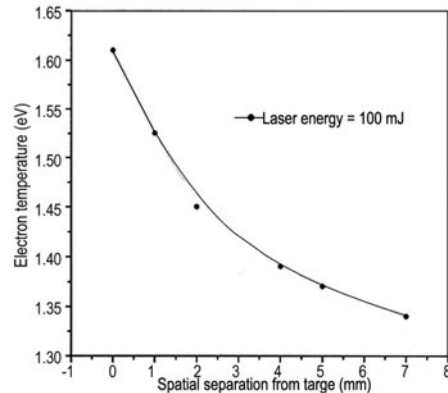


Fig.2 T_e distribution in plasma at 100 mJ

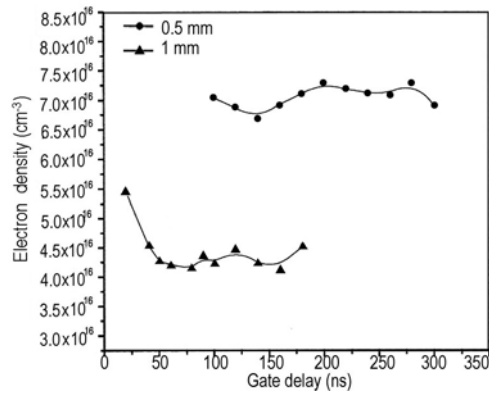


Fig.3 Temporal evolution of n_e (Energy of laser beam = 100 mJ)

For the time resolved measurement, a time window of 30 ns is selected to get an optimum resolution. The temporal variations of electron density near the target, at distances of 0.5 mm and 1 mm from the target are discussed. The electron number density is estimated from Stark broadening of Ti II ($3d^2.4s-3d^2.4p$) transition at 350.5 nm. The observed decay of electron density close to the target and at a spatial separation of 1 mm is plotted in Fig. 3. The temporal variation of n_e in the case of 1 mm distance has a fast rise up to a maximum value (5.45×10^{16}), which decays to lower values at larger gate delays. The rising part is so fast that it cannot be recorded because of the constraints in the present experimental setup. Here, we observe the high density plasma front, indicated by the intense continuum emission, followed by lower density plasma at a later time. For delays greater than 50 ns, there is very little change in n_e values. Similar is the case for 0.5 mm also. The observation is probably due to the recombination processes. The relatively low value at 1 mm with respect to that of 0.5 mm can be attributed to the plasma propagation^[9,10]. The spatio-temporal evolution of density at an increased energy (200 mJ) is as given in Fig. 4. At the increased laser energy, the density is higher at 1 mm. A weak time-dependence of density is seen around 3 mm. At a distance of 4 mm, there is some kind of modulating dependence of n_e with a time delay.

The time evolution of line intensities is extracted within a time range extending up to 300 ns after the

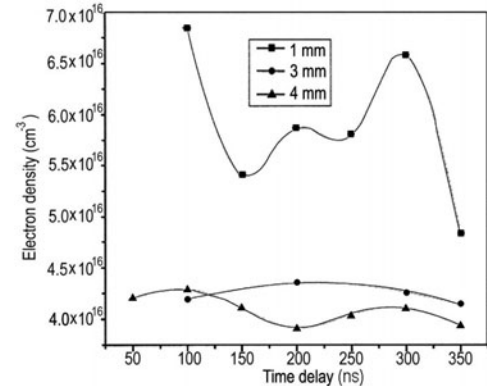


Fig.4 Spatio-temporal electron density evolution in plasma at 200 mJ

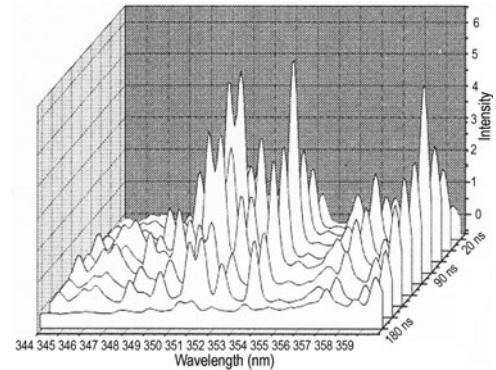
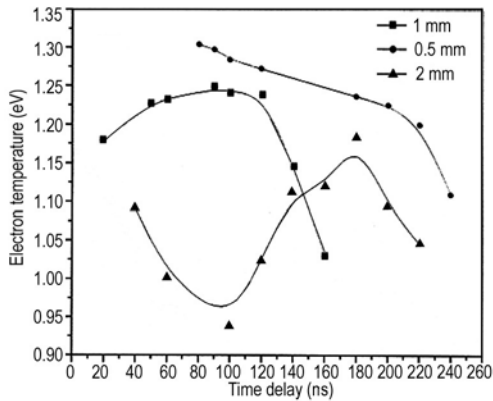
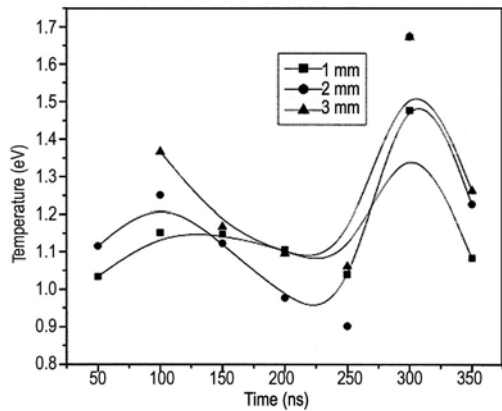


Fig.5 Temporal evolution of a typical Ti spectrum at distance 1 mm from the target

plasma initiation. The typical temporal spectra evolution is shown in Fig. 5. The majority of the emissions are from Ti I and Ti II. The spectral line kinetics of (a) 343.93(Ti I), (b) 347.80(Ti I), (c) 349.10(Ti II), (d) 350.50(Ti II), (e) 351.08(Ti II), (f) 352(Ti II), (g) 353.50(Ti II), (h) 357.30(Ti II), (i) 358.70(Ti II), (j) 359.60(Ti II) are presented. By the analysis of this figure, it is possible to observe the initial spectral continuum, essentially due to collisions of free electrons with heavy particles and radiative recombination of electrons with positive ions. Each fragment of the spectra belongs to a different portion of the LIP temporal distribution. The emission lines become progressively narrower as a consequence of the electron number distribution. It points out that the excitation temperatures must decrease during the time evolution^[9]. The maximum intensity is reached after a characteristic time of 90 ns, which depends on the observation distance and this represents the most populated section of LIP. As a consequence of the high ionization degree, for most part of the spectra, the ionic lines are proportionally more intense than those of the atoms, while on the tail of the temporal distribution of LIP intensities, which correspond to the colder part of the plasma, it is possible to observe the progressive disappearance of atomic lines^[6,7].

The electron temperature distribution within this range of time is also calculated. The farther the observation distance from the target, the colder is the

**Fig.6** T_e evolution at 100 mJ as a function of time**Fig.7** Distribution of electron temperature at a laser energy of 200 mJ

plasma, as depicted in Fig. 6. This may be due to the expansive dissipation of the plume energy. At a distance of 1 mm, the temperature of the tail of the temporal distribution falls down to 1 eV from the initial value of 1.2 eV. At 0.5 mm from the target, the initial temperature is higher than this. At farther distances, the temperature begins to rise at later times. This can be attributed to the recombination processes which compensate for the expansive cooling. With laser energy of 200 mJ, the evolved temperature is shown in Fig. 7. The sudden electron temperature increase at 300 ns is due to the laser energy absorption that occurs during the laser-plasma interaction. This can be explained by atom-atom collisions at larger distances from the target^[11]. Such an increase can flourish only with tolerable decay rates. Even at a 3 mm distance, the recombination rate is not dominant and the increased electron temperature shows a faster decay.

We confirm the validity of the McWhirter criterion^[12] in the present experiment, which states that the minimum density of LTE should be, $n_e \geq 1.4 \times 10^{14} T_e^{1/2} (\Delta E)^3 \text{ cm}^{-3}$ with T_e and ΔE in eV. For the transition with the largest energy gap of 3.574 eV, applying the peak plume temperature of 1.67 eV to this criterion predicts a lower limit for n_e of $8.25 \times 10^{15} \text{ cm}^{-3}$. Our observed n_e values are always larger than this lower bound, implying that the LTE approximation assumed for our analysis is valid.

4 Conclusions

Within the range of laser fluence and temperature studied, excited atomic species of Ti II are prominent in the LIP from TiO_2 target. Spectral lines of oxygen or molecular species were not observed under the present experimental conditions. The majority of the emissions were due to Ti II during the interval of 0 ns to 180 ns. At a spatial separation of 1 mm from the target, the most populated section of LIP emerged after 90 ns. Variation of n_e and T_e obtained by time integrated and time resolved spectroscopic techniques were verified and tested for the validity of LTE and found to satisfy the necessary criterion for LTE. In conclusion, we can see that LIP from TiO_2 target, under the present experimental conditions, validates LTE.

5 Acknowledgments

VJD is thankful to CELOS, CUSAT (Cochin) and UGC (Government of India), New Delhi for financial support and Dr Jaimon Yohannan, Department of Electronics, CUSAT for the help rendered towards preparing targets for the experiment.

References

- 1 Giacomo De, Shkhatov V A, Pascale O De. 2001, Spectrochim Acta PART B, 56: 753
- 2 Colonna G, Casavolla A, Capitelli M. 2001, Spectrochim Acta PART B, 56: 567
- 3 Hermann J, Thomann A L, Boulmer-Leborgne C, et al. 1995, J. Appl. Phys., 77: 2928
- 4 Dann V J, Mathew Manoj V, Nampoori V P N, et al. Temporal profile of Ti in laser produced plasma from Titania. Proceedings of Fifth National Laser Symposium, (Vellore Institute of Technology, Vellore, India, December 7-10, 2005)
- 5 Hermann J, Boulmer-Leborgne C, Hong D. 1998, J. Appl. Phys., 83: 691
- 6 Restrepo E, Devia A. 2004, J. Vac. Sci. Tech., A 22: 377
- 7 Singh R K, Holland O W, Narayan J. 1990, J. Appl. Phys., 68: 233
- 8 Harilal S S, O'Shay Beau, Tillack Mark S. 2005, J. Appl. Phys., 98: 13306
- 9 Giacomo A De. 2003, Spectrochim Acta PART B, 58: 71
- 10 Giacomo A De, Shkhatov V A, Senesi G S, et al. 2001, Spectrochim Acta PART B, 56: 1459
- 11 Gordillo-Vazquez F J, Perea A, Chaos J A, et al. 2001, Appl. Phys. Lett., 78: 7
- 12 Bekefi G. 1976, Principles of Laser Plasmas. (New York: Wiley)

(Manuscript received 29 August 2006)

E-mail address of V J DANN: dannvj@cusat.ac.in